*Research Article*

# Enhanced Myocardial Tissue Visualization: A Comparative Cardiovascular Magnetic Resonance Study of Gradient-Spin Echo-STIR and Conventional STIR Imaging

**Sadegh Dehghani** [iD],[1] **Shapoor Shirani** [iD],[2] **and Elahe Jazayeri Gharebagh** [iD][1]

[1]*Radiation Sciences Department, School of Allied Medical Sciences, Tehran University of Medical Sciences, Tehran, Iran*
[2]*Tehran Heart Center, Tehran University of Medical Sciences, Tehran, Iran*

Correspondence should be addressed to Sadegh Dehghani; dehghan907@gmail.com

*Purpose*. This study is aimed at evaluating the efficacy of the gradient-spin echo- (GraSE-) based short tau inversion recovery (STIR) sequence (GraSE-STIR) in cardiovascular magnetic resonance (CMR) imaging compared to the conventional turbo spin echo- (TSE-) based STIR sequence, specifically focusing on image quality, specific absorption rate (SAR), and image acquisition time. *Methods*. In a prospective study, we examined forty-four normal volunteers and seventeen patients referred for CMR imaging using conventional STIR and GraSE-STIR techniques. Signal-to-noise ratio (SNR), contrast-to-noise ratio (CNR), image quality, $T_2$ signal intensity (SI) ratio, SAR, and image acquisition time were compared between both sequences. *Results*. GraSE-STIR showed significant improvements in image quality ($4.15 \pm 0.8$ vs. $3.34 \pm 0.9$, $p = 0.024$) and cardiac motion artifact reduction (7 vs. 18 out of 53, $p = 0.038$) compared to conventional STIR. Furthermore, the acquisition time ($27.17 \pm 3.53$ vs. $36.9 \pm 4.08$ seconds, $p = 0.041$) and the local torso SAR (<13% vs. <17%, $p = 0.047$) were significantly lower for GraSE-STIR compared to conventional STIR in short-axis plan. However, no significant differences were shown in $T_2$ SI ratio ($p = 0.141$), SNR ($p = 0.093$), CNR ($p = 0.068$), and SAR ($p = 0.071$) between these two sequences. *Conclusions*. GraSE-STIR offers notable advantages over conventional STIR sequence, with improved image quality, reduced motion artifacts, and shorter acquisition times. These findings highlight the potential of GraSE-STIR as a valuable technique for routine clinical CMR imaging.

## 1. Introduction

Advances in cardiovascular magnetic resonance (CMR), using short tau inversion recovery (STIR), have allowed for the visualization of regional and global myocardial edema in various heart diseases [1, 2]. The conventional STIR, as a $T_2$-weighted turbo spin echo ($T_2$-w TSE) or edema imaging technique, uses a third inversion pulse following a double inversion recovery (DIR) black-blood preparation to additionally null the fat signal [3, 4]. Therefore, by using triple inversion recovery (TIR), conventional STIR black-blood technique aids to diagnose acute myocardial lesions more precisely [5, 6]. In this technique, given the nonspectrally selective third inversion pulse, the signal generated by water protons in the myocardium is also inverted, resulting in an improved contrast-to-noise ratio (CNR). As a result, it enhances the differentiation between edematous tissue and normal myocardium [7, 8]. However, the conventional STIR is TSE-based sequence with TSE factor = 25-35. High TSE factors present several challenges in this technique, including increased sensitivity to slow-flow artifacts around the endocardial borders, resulting in elevated signal intensity (SI) [9, 10], and cardiac motion artifacts [11]. Moreover, a high TSE factor is subject to high specific absorption rate (SAR) [12].

In response to these challenges, gradient-spin echo (GraSE) technique may offer an alternative to conventional TSE imaging, potentially offering advantages such as faster image acquisition and reduced energy deposition. The GraSE technique is a fast MRI method that combines

elements of the TSE and echo planar imaging (EPI) techniques. It involves generating a series of spin echoes using multiple 180° refocusing radiofrequency (RF) pulses, where gradient echoes are sampled before and after each spin echo with an EPI readout [13]. By employing EPI as a gradient-echo (GRE) readout technique, leading to increased speed in TSE sequences, the energy deposition in the patient can be reduced [14]. Furthermore, the acquisition time will be reduced, resulting in lower cardiac motion artifacts, particularly for patients with irregular breathing patterns [15].

Therefore, the aim of our study was to systematically compare the efficacy of GraSE-STIR and conventional STIR techniques in both normal volunteers and patients diagnosed with cardiac edema. Our objective was to evaluate the influence of the GraSE technique on various key parameters including image quality, safety parameters such as SAR, and image acquisition time.

## 2. Methods

The local ethic committee approved this prospective study, and written informed consent was obtained from all volunteers prior to CMR imaging. All scans were performed using a 1.5-tesla (T) MRI system (Ingenia, Philips Medical Systems, Best, The Netherlands) with a maximum gradient strength of 45 mT/m and a maximum slew rate of 200 mT/m/ms. A 32-channel torso coil with digital interface was used for signal reception. Exclusion criteria included magnetic resonance incompatible implants, severe claustrophobia, and general contraindications to MRI, clinical instability, and severe artifacts in desired images, leading to bias in qualitative and quantitative measurement. And patients with myocardial edema disease were included.

*2.1. Study Cohort.* As shown in Figure 1, we assessed forty-four normal volunteers (mean age of $44.8 \pm 19.6$ years, 20 females and 24 males) with no cardiac disease history. Furthermore, seventeen patients with cardiac edema disease were included to this study (mean age of $41.7 \pm 14.8$ years, 7 female patients and 10 males). Participants were scanned with both conventional STIR and GraSE-STIR protocols, in random order, for the purposes of comparing $T_2$ SI ratio, SNR, CNR, image quality, and artifacts. Of these fifty-three volunteers, CNR was only calculated in eleven patients who had focally increased SI in edema imaging techniques. Characteristics of patients are summarized in Table 1.

*2.2. MRI Protocol.* The imaging protocol included cine, using balanced steady-state free precession (bSSFP), conventional STIR, and GraSE-STIR sequences at standardized apical, midcavity, and basal short-axis (SAX) levels [16], covering 16 segments of the 17-segment model as recommended by the American Heart Association (AHA) [17], two chamber (2CH), three chamber (3CH), and four chamber (4CH) plans. The late gadolinium enhancement (LGE) imaging was also done for patients with cardiac disease. All images were acquired, using the following parameters: for bSSFP and LGE, acquired pixel size = $1.8 \times 2.3$ mm, reconstructed pixel slice = $1.5 \times 1.5$ mm, and slice thickness = 8 mm during
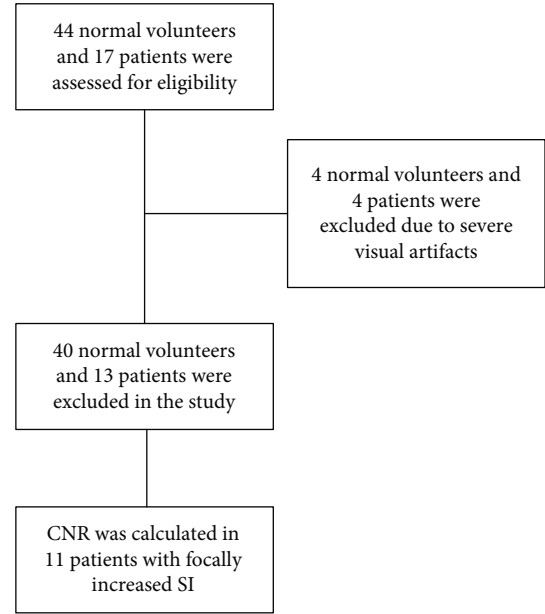


Figure 1: Flowchart depicting participant selection.

Table 1: Characteristics of patients.

| Parameters | Results |
| --- | --- |
| Number of normal volunteers (females/males) | 44 (20/24) |
| Age (years) | $44.8 \pm 19.6$ |
| Number of patients (females/males) | 17 (7/10) |
| Age (years) | $41.7 \pm 14.8$ |
| Heart rate (min$^{-1}$) | $66.13 \pm 18.57$ |
| Height (cm) | $160.73 \pm 16.47$ |
| Weight (kg) | $60.54 \pm 19.21$ |
| LV ejection fraction (%) | $53 \pm 13.5$ |
| LV end-diastolic volume/BSA (ml/m$^2$) | $68.7 \pm 16.48$ |
| LV end-systolic volume/BSA (ml/m$^2$) | $29.57 \pm 8.4$ |

LV: left ventricular; BSA: body surface area.

end-expiration breath-hold period. For cine imaging, bSSFP pulse sequence was used (TR = 3.5 ms, TE = 1.4 ms, FA = 55°, and temporal resolution ≤ 45 ms). For conventional STIR, we used a TIR black-blood turbo spin echo pulse sequence with TSE factor = 25 and TSE$_{es}$ = 5.4 ms. For GraSE-STIR, we used a TIR black-blood GraSE pulse sequence with TSE factor = 18, EPI factor = 3, and TSE echo spacing (TSE$_{es}$) = 7.4 ms. Other parameters, including TR = 2 heartbeat, TE = 80 ms, TI = 165 ms, slice thickness = 10 mm, field of view (FOV) = 270 × 270 mm, matrix size = 124 × 122, acceleration factor = 1.4, shot duration = 134 ms, volume shimming, and bandwidth = 204 Hz/pixel, were the same for both sequences. In the case of patients with cardiac disease, eight minutes after intravenous application of a standard MRI contrast agent (DOTAREM, 0.4 mmol/kg), look-locker sequence was performed with increasing TI to achieve the nulling of normal myocardium. After that, definitive LGE images were acquired with an

IR-prepared gradient-echo technique (TR = 4.5 ms, TE = 1.8 ms, and FA = 15), using the TI that allowed for the best nulling of normal myocardium.

### 2.3. Image Analysis

*2.3.1. $T_2$ SI Ratio Measurement.* To assess the presence of edema, the $T_2$ SI ratio of left ventricular (LV) myocardium to skeletal muscle was calculated for all $T_2$-w images with Philips extended MR workspace (version 2.6.3.4; Philips Medical Systems, Best, The Netherlands). According to a previous study [2], a $T_2$ SI ratio equal to or above a threshold of two was considered to be positive for the presence of edema. Calculation of the $T_2$ SI ratio involved manually tracing region of interest (ROI) contours in different plans of the conventional STIR and GraSE-STIR images. In every plan, five ROIs were traced on different parts of LV myocardium and five ROIs on skeletal muscles, and then, the mean SI for LV myocardium and skeletal muscle was calculated. In the presence of edema, we measured the $T_2$ SI ratio in a single myocardial slice per patient, specifically in the slice with the most extensive regional edema. To avoid slow-flow artifacts, ROIs were traced by carefully omitting the inner endocardial border. In all $T_2$-w images, skeletal muscle was identified as cross-referenced by cine images in the same slice position. The mean SI of the LV myocardium was divided by the mean SI of skeletal muscle in the same slice resulting in a $T_2$ SI ratio [18].

*2.3.2. CNR Measurement.* Relative CNR was calculated in patients who had evidence of regional SI increase in $T_2$-w images, representing edema. The mean SI of the edematous region was subtracted from the mean SI of remote myocardium and divided by the mean standard deviation (SD) of background noise [19]. The mean SD of background noise was obtained by tracing a ROI in air 2–3 cm anterior to the chest wall [20]. CNR was only performed in one myocardial slice per patient, where the greatest extent of regional edema was present.

In order to compare slow-flow artifact suppression between conventional STIR and GraSE-STIR, CNR was calculated between myocardium and blood. The LV myocardial mean SI was subtracted from the mean SI of blood within the LV myocardium and divided by the mean SI of blood [19].

*2.3.3. SNR Measurement.* Relative SNR was calculated for conventional STIR and GraSE-STIR images. For calculating SNR, the mean SI of LV myocardium was divided by the mean SD of the background noise for each slice [20].

*2.3.4. Image Quality Analysis.* Two experienced CMR observers, each with over 5 and 8 years of experience, independently and blindly assessed $T_2$-w images from patients. Their analysis involved the qualitative evaluation of myocardial border clarity, as well as the identification of artifacts, including high SI at the subendocardial border of the LV myocardium, posterolateral signal loss, and cardiac motion that might affect the LV myocardium assessment and interpretation. Image quality was scored using the following 5-point rating scale [21]: 1 represented severe image distortion from artifacts that

significantly limited interpretation, 2 indicated significant impairment due to artifacts, 3 denoted moderate artifact impairment, 4 reflected mild artifact impairment, and 5 represented images without impairment from artifacts. In cases where a consensus could not be reached between the two radiologists, a third radiologist with ten years of experience in cardiac MRI was consulted to resolve the issue. Additionally, the above-mentioned artifacts were assessed separately, identifying the presence of any artifact in each image, and the number of patients exhibiting each type of artifact was calculated. Finally, the scan time required for both conventional STIR and GraSE-STIR sequences was evaluated.

*2.4. Inter- and Intrarater Repeatability.* In this study, the intrarater repeatability was calculated from two independent evaluations of all subjects by a single observer, separated by one month, and it was expressed as an intraclass correlation coefficient (ICC). Furthermore, the interrater reliability coefficient (IRR) was used to show the agreement among raters as a basis for our calculation [22].

*2.5. Statistical Analysis.* Data analysis was done using Origin pro 2022 version. Descriptive statistics, such as means, SD, and confidence intervals, were calculated. Paired $t$-tests were used to assess differences between the sequences. The Pearson rank correlation analyses were conducted to evaluate the associations between image qualities measured by observers. Kappa values were those between 0 and 0.40, poor agreement; those between 0.41 and 0.75, good agreement; and those between 0.76 and 1.00, excellent agreement [23].

## 3. Results

$T_2$-w imaging was done, using conventional STIR and GraSE-STIR sequences. Eight volunteers (4 normal volunteers and 4 patients) were excluded from analysis due to noneligible visual artifacts, including cardiac motion (3 cases), respiratory motion (2 cases), or both (3 cases), observed in both sequences. The remaining forty normal volunteers and thirteen patients formed the study group for measuring of GraSE-STIR performance.

*3.1. Image Quality Analysis.* Significant improvement in image quality was observed with GraSE-STIR compared to conventional STIR sequence ($4.15 \pm 0.8$ vs. $3.34 \pm 0.9$, $p = 0.024$). The assessment of intra- and interreader agreement for both sequences revealed very good agreement between repeated readings of the same reader (ICC > 0.74) and between the measurements of different readers (IRR > 0.71). Figure 2 shows high-quality images of conventional STIR and GraSE-STIR sequences from normal volunteer.

*3.2. Artifact Measurement.* High SI artifacts due to the slow flow of blood next to the endocardium in LV myocardium were observed in twenty-six and twenty-four out of fifty-three volunteers in conventional STIR and GraSE-STIR, respectively, with no significant differences ($p = 0.078$). As shown in Figure 3, cardiac motion artifact was significantly higher in conventional STIR compared to GraSE-STIR sequence (18 vs. 7 out of 53, $p = 0.038$). Posterolateral loss
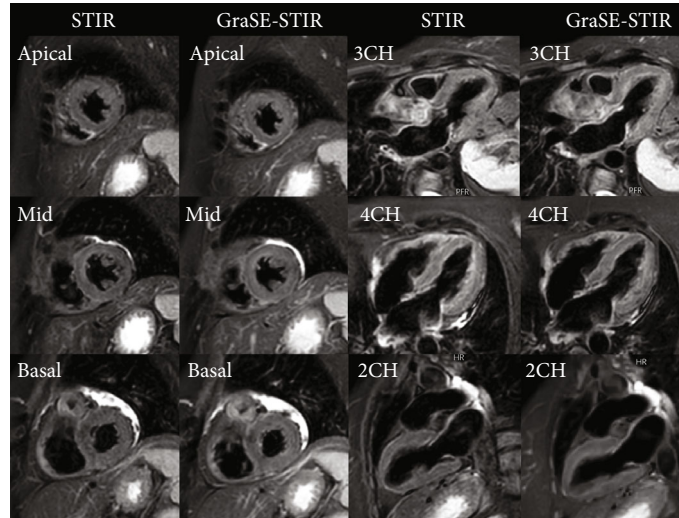
FIGURE 2: GraSE-STIR and conventional STIR images of normal male volunteer. Image quality analysis represented high-quality images (scale of 5 for both techniques) for both sequences.

of signal in conventional STIR (3 out of 53) and GraSE-STIR (5 out of 53) sequences did not show any statistical differences ($p = 0.082$).

### 3.3. Quantitative Analysis

*3.3.1. $T_2$ SI Ratio.* The $T_2$ SI ratio between myocardial edema and musculoskeletal muscle was achieved at $2.5 \pm 1.2$ for conventional STIR and $2.4 \pm 0.8$ for GraSE-STIR sequence. No significant differences were observed between these two sequences, and good correlations were obtained between both techniques ($p = 0.71$, ICC = 0.64, IRR = 0.56). $T_2$ SI ratios were also measured between normal myocardium and musculoskeletal muscle for both sequences in all planes. $T_2$ SI ratios and Pearson's correlations are summarized in Table 2. No significant differences were found between both sequences ($p = 0.141$). Additionally, a good correlation was achieved between sequences (ICC = 0.70 – 0.80, IRR = 0.62 – 0.72).

*3.3.2. CNR Measurement.* In patients with regional myocardial edema, CNR between edema and remote normal myocardium demonstrated no significant difference between GraSE-STIR ($116 \pm 14.51$) and conventional STIR ($108 \pm 20$) sequences with a $p$ value of 0.068. Furthermore, CNR between myocardium and blood showed no significant differences between two sequences ($8.36 \pm 5.12$ vs. $9.5 \pm 4.21$, $p = 0.052$). Figure 4 shows CMR images of the patient with myocardial edema.

*3.3.3. SNR Measurement.* SNR of conventional STIR sequence for all plans was calculated as follows: apical, $179 \pm 13.61$; midventricle, $180 \pm 12.5$; basal, $182 \pm 13.17$; 2CH, $177.55 \pm 9.78$; 3CH, $175.87 \pm 12.23$; and 4CH, $181.38 \pm 10.15$. No significant differences were shown across all plans ($p = 0.116$). SNR of GraSE-STIR sequence was calculated as follows: apical, $176 \pm 9.23$; midventricle, $180.24 \pm 8.17$; basal, $174 \pm 9.18$; 2CH, $179.78 \pm 11.48$; 3CH, $180 \pm 9.97$; and 4CH, $177.31 \pm 9.69$. No significant differences were shown across all plans ($p = 0.106$). Furthermore, no significant

differences were shown between two sequences ($p = 0.093$, Figure 5(a)).

*3.3.4. Acquisition Time Measurement.* The acquisition time for every plan of 2CH, 3CH, and 4CH was 6-8 seconds for GraSE-STIR sequence and 8-12 seconds for conventional STIR without any significant differences ($p = 0.061$). However, as demonstrated in Figure 5(b), the mean duration of time taken for GraSE-STIR and conventional STIR sequences was $27.17 \pm 3.53$ and $36.9 \pm 4.08$ seconds, respectively, in SAX plans with statistically significant difference ($p = 0.041$).

*3.3.5. SAR Measurement.* In conventional STIR imaging, SAX view, SAR was measured to be less than 0.4 W/kg, and the local torso SAR was successfully limited to less than 17%. However, in GraSE-STIR imaging, SAR was achieved less than 0.3 W/kg, and local torso SAR was limited to less than 13%. Our statistical analysis revealed no significant differences in SAR ($p = 0.071$). Local torso SAR was statistically lower in GraSE-STIR sequence ($p = 0.047$). No variation was found for SAR (<0.3 W/kg) and local torso SAR (<10%) in 2CH, 3CH, and 4CH for both STIR and GraSE-STIR sequences ($p = 1.00$).

## 4. Discussion

The utilization of CMR has revolutionized the understanding and diagnosis of myocardial pathologies, offering noninvasive insights into tissue characteristics. One key aspect in CMR imaging is the accurate visualization of myocardial edema using STIR technique, which aids in differentiating acute from chronic myocardial lesions. However, the conventional STIR black-blood technique, though widely employed, has been associated with varying image quality, raising concerns about its diagnostic reliability in clinical practice [5, 6].
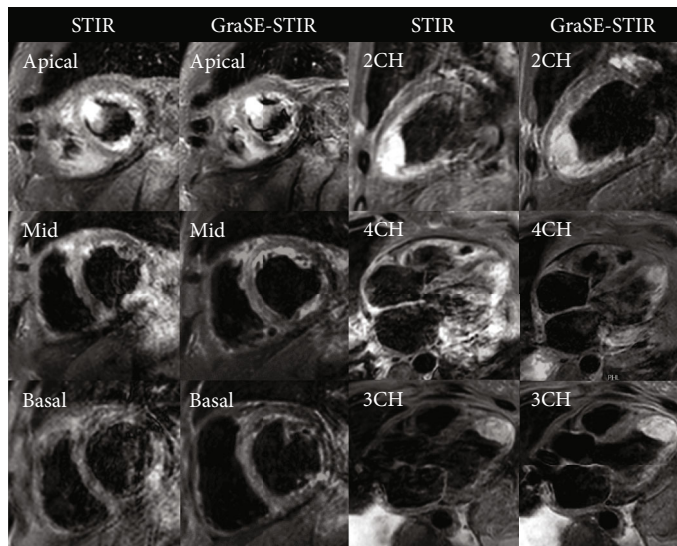
FIGURE 3: GraSE-STIR and conventional STIR images of the patient with severely enlarged size and reduced systolic function. Large semimobile clot with edema can be seen in apical section. The image quality of GraSE-STIR (scale of 4 out of 5) is significantly higher than conventional STIR sequence (scale of 3 out of 5). Motion artifact is clearly seen in 2CH and 4Ch of conventional STIR images. High SI artifacts in LV myocardium are clearly seen in SAX, 2CH, and 4CH plans of both sequences with no significant differences.

TABLE 2: Quantitative analysis of $T_2$ signal intensity (SI) ratio of normal myocardial tissue.

| $T_2$ signal intensity ratio | Conventional STIR | GraSE-STIR | Intrarater correlation (ICC) | Interrater correlation (IRR) |
| --- | --- | --- | --- | --- |
| Basal | $1.79 \pm 0.2$ | $1.77 \pm 0.17$ | 0.71 | 0.62 |
| Midventricle | $1.76 \pm 0.15$ | $1.75 \pm 0.21$ | 0.77 | 0.65 |
| Basal | $1.78 \pm 0.18$ | $1.74 \pm 0.23$ | 0.80 | 0.72 |
| 2CH | $1.77 \pm 0.16$ | $1.79 \pm 0.16$ | 0.75 | 0.68 |
| 3CH | $1.81 \pm 0.13$ | $1.77 \pm 0.14$ | 0.7 | 0.62 |
| 4CH | $1.81 \pm 0.14$ | $1.79 \pm 0.2$ | 0.72 | 0.66 |
| Global | $1.78 \pm 0.17$ | $1.77 \pm 0.19$ | 0.7 | 0.65 |

Given the faster acquisition of images with the GraSE technique compared to TSE, our study is aimed at evaluating the performance of GraSE-based STIR sequences in CMR imaging compared to conventional TSE-based STIR sequences. By investigating key parameters such as image quality, motion artifacts, acquisition time, and safety parameters, our goal was to provide valuable insights into the potential clinical utility of GraSE-STIR in visualizing myocardial tissue.

4.1. Image Quality Analysis. Image quality indeed plays an important role in achieving accurate diagnoses of edema disease [24]. Despite its clinical utility, the STIR sequence is often limited by artifacts, including inadequate blood suppression for slow blood flow near wall motion abnormalities. Additionally, the long acquisition time using a TSE readout can introduce motion artifacts, particularly in tachyarrhythmia patients [25, 26]. Therefore, it is important to highlight the significant improvement in image quality and motion artifact reduction achieved by GraSE-STIR when compared to conventional STIR. In this study, the excellent agreement

between independent observers reinforced the reliability of the GraSE-STIR technique in producing consistent image quality. Additionally, GraSE-STIR maintained comparable values for slow-flow artifact and posterolateral signal loss when compared to conventional STIR. This suggests that GraSE-STIR can provide detailed tissue information compared to conventional STIR. Several studies have demonstrated that GraSE sequence plays a crucial role in accurately measuring $T_2$ values in CMR imaging compared to the conventional TSE technique [20, 21, 27]. Its excellent reproducibility in quantification, even in the presence of rapidly moving heart structures, emphasizes its potential to enhance diagnostic capabilities and streamline imaging protocols in cardiovascular imaging studies. Moreover, another research has shown that the GraSE sequence, through a long signal readout, provides $T_2$-weighted contrast, essential for various clinical applications such as MR cholangiopancreatography (MRCP) which confirmed our results [28]. Additionally, GraSE imaging has been found to reduce scan time for brain imaging and has a potential for clinical use in patients with brain disorders [29, 30]. Notably, in our study,
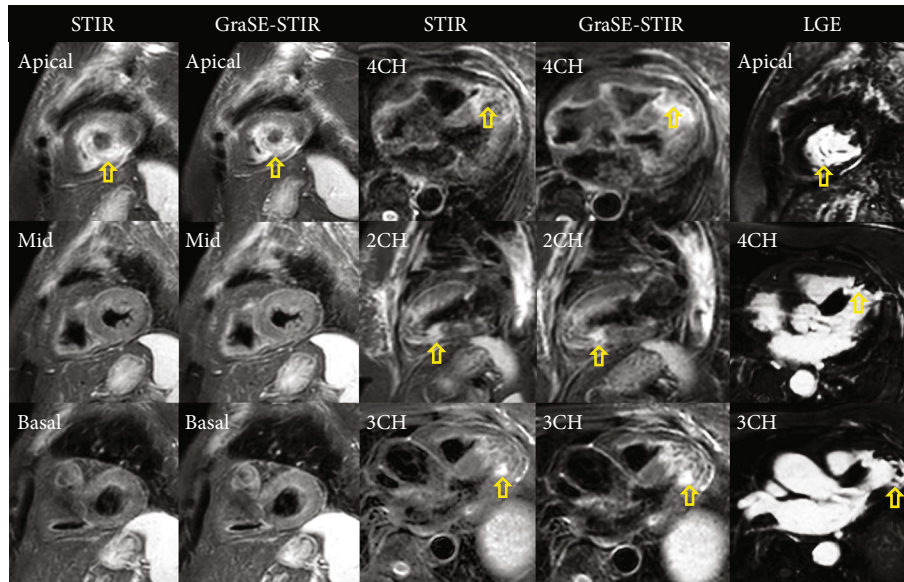
FIGURE 4: The comparison of myocardial edema imaging techniques. GraSE-STIR, conventional STIR, and late gadolinium enhancement (LGE) of myocardial edema in the patient with normal left ventricle (LV) size, reduced systolic dysfunction, and apical segment aneurysm formation with layered apical clot. Regional edema is defined by areas of increased SI (arrows) in all sequences.
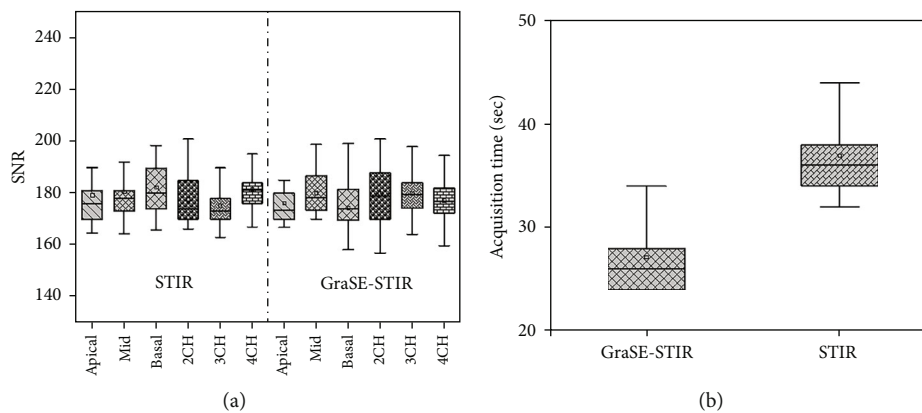


(a)

(b)

FIGURE 5: Quantitative analysis of conventional STIR and GraSE-STIR in CMR imaging. (a) Signal-to-noise ratio (SNR) of conventional STIR and GraSE-STIR. No significant differences were found among different planes for conventional STIR ($p = 0.116$) and GraSE-STIR ($p = 0.106$) as well as between both sequences ($p = 0.093$). (b) Time taken for conventional STIR was significantly higher than GraSE-STIR in short-axis (SAX) view ($p = 0.041$).

GraSE-STIR showed significantly shorter acquisition times in the SAX view compared to conventional STIR, resulting in markedly improved image quality.

4.2. Quantitative Analysis. The $T_2$ SI ratio for conventional STIR and GraSE-STIR sequences in all plans for participants without edema remained within the normal range, with no significant differences. Furthermore, the $T_2$ SI ratio between myocardial edema and musculoskeletal showed no significant differences that was aligned with previous studies [31, 32]. This provides the assurance that GraSE-STIR maintains image quality standards. In our study, the same SNR observed with GraSE-STIR, compared to conventional STIR, across different myocardial segments highlights its efficacy

in capturing detailed tissue information like conventional STIR. Furthermore, the same CNR observed in patients with regional myocardial edema further emphasizes the diagnostic potential of GraSE-STIR, similar to conventional STIR. Bagnato et al. [33] showed that GraSE sequences with EPI factor/TE = 3/50 and 3/75 ms were comparable to the $T_2$-w TSE technique for measuring the CNR between white matter lesions and normal-appearing white matter as well as detection of white matter lesions. Another study done by Yoshida et al. [34] demonstrated that conducting 3.0 T MRCP using the GraSE sequence within a single breath-hold significantly enhanced the CNR of the common bile duct. This advancement was accomplished with an impressive 95% reduction in acquisition time compared to conventional three dimensional

(3D) MRCP employing 3D TSE. These findings emphasize the reliability and reproducibility of the GraSE technique for edema imaging.

*4.3. SAR and Local Torso SAR Measurements.* A crucial aspect of MRI studies is SAR, reflecting energy deposition in the patient's tissue during scans. SAR reduction is especially beneficial in scenarios involving repeated or extended imaging, minimizing tissue heating and patient discomfort [35]. Our findings demonstrate that the GraSE-STIR sequence not only offered enhanced image quality but also exhibited a reduction in local torso SAR in SAX view compared to the conventional STIR sequence. Although no significant differences were observed between GraSE-STIR and conventional STIR in terms of SAR, this difference can be significant in higher magnetic fields. It is important to note that at higher magnetic fields (e.g., 7 T), obtaining $T_2$-w TSE images in vivo is not possible due to the high SAR [33]. Therefore, techniques reducing the SAR without compromising image quality could be a potential alternative for TSE-based techniques. Okanovic et al. [36] and Chu et al. [37] also confirmed our work. They indicated high-quality, artifact-free images with a significant SAR reduction in GraSE in magnetic fields exceeding 3 T compared to TSE sequence.

## 5. Limitations

Firstly, it was conducted at a single center utilizing a specific MRI scanner, potentially constraining the broader applicability of our edema imaging methodology. Multicenter studies are needed to validate the reproducibility and transferability of our findings. Secondly, the sample size in our study was small, primarily due to the long acquisition time required for CMR scans. This limited our ability to incorporate a larger cohort of volunteers. Thirdly, most of the volunteers were normal with approximately normal heart rate. This technique can be evaluated better in tachyarrhythmia patients with severe cardiac motion artifact. Fourthly, these two techniques were compared in a 1.5 T MRI scanner, while at higher magnetic fields, GraSE-STIR and conventional STIR may be more comparable in terms of SAR. Finally, the inclusion of specific patient and volunteer populations (e.g., those with certain cardiac conditions or imaging contraindications) may have influenced the results. Therefore, more strategies must be considered to mitigate selection bias in future research. These limitations highlight the need for future research to address these gaps and provide a more comprehensive understanding of edema imaging in different populations.

## 6. Conclusion

Our study demonstrates that the GraSE-STIR approach provides not only improved image quality and reduced motion artifacts but also lowers local torso SAR compared to conventional STIR imaging. These findings emphasize the safety and feasibility of implementing GraSE-STIR in clinical settings, offering enhanced patient comfort during scanning procedures. By addressing both diagnostic and safety concerns, GraSE-STIR emerges as a promising technique for myocardial tissue characterization in CMR imaging.

## Data Availability

All data are available on reasonable request to the corresponding author.

## Disclosure

A preprint has previously been published by Dehghani et al. [38].

## Conflicts of Interest

The authors declare that they have no conflicts of interest.

## References

[1] H. N. Skouri, G. W. Dec, M. G. Friedrich, and L. T. Cooper, "Noninvasive imaging in myocarditis," *Journal of the American College of Cardiology*, vol. 48, pp. 2085–2093, 2006.

[2] H. Abdel-Aty, A. Zagrosek, J. Schulz-Menger et al., "Delayed enhancement and T2-weighted cardiovascular magnetic resonance imaging differentiate acute from chronic myocardial infarction," *Circulation*, vol. 109, no. 20, pp. 2411–2416, 2004.

[3] H. Abdel-Aty, O. Simonetti, and M. G. Friedrich, "T2-weighted cardiovascular magnetic resonance imaging," *Journal of Magnetic Resonance Imaging: An Official Journal of the International Society for Magnetic Resonance in Medicine*, vol. 26, no. 3, pp. 452–459, 2007.

[4] O. P. Simonetti, J. P. Finn, R. D. White, G. Laub, and D. A. Henry, ""Black blood" T2-weighted inversion-recovery MR imaging of the heart," *Radiology*, vol. 199, no. 1, pp. 49–57, 1996.

[5] A. R. Payne, M. Casey, J. McClure et al., "Bright-blood T2-weighted MRI has higher diagnostic accuracy than dark-blood short tau inversion recovery MRI for detection of acute myocardial infarction and for assessment of the ischemic area at risk and myocardial salvage," *Circulation Cardiovascular Imaging*, vol. 4, no. 3, pp. 210–219, 2011.

[6] M. Henningsson, S. Malik, R. Botnar, D. Castellanos, T. Hussain, and T. Leiner, "Black-blood contrast in cardiovascular MRI," *Journal of Magnetic Resonance Imaging*, vol. 55, no. 1, pp. 61–80, 2022.

[7] G. Krinsky, N. M. Rofsky, and J. C. Weinreb, "Nonspecificity of short inversion time inversion recovery (STIR) as a technique of fat suppression: pitfalls in image interpretation," *AJR American Journal of Roentgenology*, vol. 166, no. 3, pp. 523–526, 1996.

[8] A. Jackson, S. Sheppard, A. C. Johnson, D. Annesley, R. D. Laitt, and A. Kassner, "Combined fat- and water-suppressed MR imaging of orbital tumors," *AJNR American Journal of Neuroradiology*, vol. 20, no. 10, pp. 1963–1969, 1999.

[9] R. W. Brown, Y.-C. N. Cheng, E. M. Haacke, M. R. Thompson, and R. Venkatesan, *Magnetic Resonance Imaging: Physical Principles and Sequence Design*, vol. 16, John Wiley & Sons, New York, 2014.

[10] D. Filomena, T. Dresselaers, and J. Bogaert, "Role of cardiovascular magnetic resonance to assess cardiovascular

inflammation," *Frontiers in Cardiovascular Medicine*, vol. 9, article 877364, 2022.

[11] K. Oshio and D. A. Feinberg, "GRASE (gradient-and spin-echo) imaging: a novel fast MRI technique," *Magnetic Resonance in Medicine*, vol. 20, no. 2, pp. 344–349, 1991.

[12] X. Peng, D. Borup, and J. Pipe, "Accelerated spiral turbo-spin-echo sequence with split spiral in-out acquisition," in *Proc Int Soc Magn Reson Med*, p. 4185, 2021.

[13] A. T. O'Brien, K. E. Gil, J. Varghese, O. P. Simonetti, and K. M. Zareba, "T2 mapping in myocardial disease: a comprehensive review," *Journal of Cardiovascular Magnetic Resonance*, vol. 24, no. 1, pp. 1–25, 2022.

[14] P. Mansfield and I. L. Pykett, "Biological and medical imaging by NMR," *Journal of Magnetic Resonance*, vol. 29, no. 2, pp. 355–373, 1978.

[15] M. He, J. Xu, Z. Sun et al., "Comparison and evaluation of the efficacy of compressed SENSE (CS) and gradient-and spin-echo (GRASE) in breath-hold (BH) magnetic resonance cholangiopancreatography (MRCP)," *Journal of Magnetic Resonance Imaging*, vol. 51, no. 3, pp. 824–832, 2020.

[16] D. R. Messroghli, G. J. Bainbridge, K. Alfakih et al., "Assessment of regional left ventricular function: accuracy and reproducibility of positioning standard short-axis sections in cardiac MR imaging," *Radiology*, vol. 235, no. 1, pp. 229–236, 2005.

[17] American Heart Association Writing Group on Myocardial Segmentation and Registration for Cardiac Imaging, M. D. Cerqueira, N. J. Weissman et al., "Standardized myocardial segmentation and nomenclature for tomographic imaging of the Heart," *Circulation*, vol. 105, no. 4, pp. 539–542, 2002.

[18] H. Abdel-Aty, P. Boyé, A. Zagrosek et al., "Diagnostic performance of cardiovascular magnetic resonance in patients with suspected acute myocarditis: comparison of different approaches," *Journal of the American College of Cardiology*, vol. 45, no. 11, pp. 1815–1822, 2005.

[19] M. S. Cocker, S. M. Shea, O. Strohm, J. Green, H. Abdel-Aty, and M. G. Friedrich, "A new approach towards improved visualization of myocardial edema using T2-weighted imaging: a cardiovascular magnetic resonance (CMR) study," *Journal of Magnetic Resonance Imaging*, vol. 34, no. 2, pp. 286–292, 2011.

[20] E. R. Hammood, S. Shirani, A. Sadri, M. Bahri, and S. Dehghani, "The role of improved motion-sensitized driven equilibrium blood suppression and fat saturation on $T_2$ relaxation time, using GraSE sequence in cardiac magnetic resonance imaging," *Journal of Magnetic Resonance Imaging*, 2023.

[21] A. M. Sprinkart, J. A. Luetkens, F. Träber et al., "Gradient spin echo (GraSE) imaging for fast myocardial T2 mapping," *Journal of Cardiovascular Magnetic Resonance*, vol. 17, no. 1, pp. 12–19, 2015.

[22] F. Del Grande, M. Delcogliano, R. Guglielmi et al., "Fully automated 10-minute 3D CAIPIRINHA SPACE TSE MRI of the knee in adults: a multicenter, multireader, multifield-strength validation study," *Investigative Radiology*, vol. 53, no. 11, pp. 689–697, 2018.

[23] J. L. Fleiss, B. Levin, and M. C. Paik, *Statistical Methods for Rates and Proportions*, John Wiley & Sons, New York, NY, 3rd edition, 2013.

[24] M. van Assen, G. Muscogiuri, D. Caruso, S. J. Lee, A. Laghi, and C. N. De Cecco, "Artificial intelligence in cardiac radiology," *La Radiologia Medica*, vol. 125, no. 11, pp. 1186–1199, 2020.

[25] D. Pennell, "Myocardial Salvage," *Circulation*, vol. 113, no. 15, pp. 1821–1823, 2006.

[26] P. Kellman, A. H. Aletras, C. Mancini, E. R. McVeigh, and A. E. Arai, "$T_2$-prepared SSFP improves diagnostic confidence in edema imaging in acute myocardial infarction compared to turbo spin echo," *Magnetic Resonance in Medicine: An Official Journal of the International Society for Magnetic Resonance in Medicine*, vol. 57, no. 5, pp. 891–897, 2007.

[27] B. Baeßler, F. Schaarschmidt, C. Stehning, B. Schnackenburg, D. Maintz, and A. C. Bunck, "Cardiac T2-mapping using a fast gradient echo spin echo sequence-first in vitro and in vivo experience," *Journal of Cardiovascular Magnetic Resonance*, vol. 17, no. 1, p. 67, 2015.

[28] M. Patel, R. Klufas, and A. Shapiro, "MR imaging of diseases of the brain: comparison of GRASE and conventional spin-echo T2-weighted pulse sequences," *AJR American Journal of Roentgenology*, vol. 165, no. 4, pp. 963–966, 1995.

[29] W. Umek, A. Ba-Ssalamah, R. Prokesch, R. Mallek, K. Heimberger, and K. Hittmair, "Imaging of the brain using the fast-spin-echo and gradient-spin-echo techniques," *European Radiology*, vol. 8, no. 3, pp. 409–415, 1998.

[30] A. J. Maubon, A. Pothin, J. M. Ferru, V. M. Berger, J. P. Daures, and J. P. Rouanet, "Unselected brain 0.5-T MR imaging: comparison of lesion detection and characterization with three T2-weighted sequences," *Radiology*, vol. 208, pp. 671–678, 1998.

[31] H. Jia, J. Guo, B. Liu, H. Meng, F. Pan, and C. Li, "Diagnostic value of 3.0 T cardiac MRI in children with suspected myocarditis: multi-parameter analysis for the evaluation of acute and chronic myocarditis," *Acta Radiologica*, vol. 61, pp. 1249–1257, 2020.

[32] Y. Zhu, D. Yang, L. Zou, Y. Chen, X. Liu, and Y.-C. Chung, "T2STIR preparation for single-shot cardiovascular magnetic resonance myocardial edema imaging," *Journal of Cardiovascular Magnetic Resonance*, vol. 21, no. 1, pp. 1–11, 2019.

[33] F. Bagnato, S. Hametner, D. Pennell et al., "7T MRI-histologic correlation study of low specific absorption rate T2-weighted GRASE sequences in the detection of white matter involvement in multiple sclerosis," *Journal of Neuroimaging*, vol. 25, no. 3, pp. 370–378, 2015.

[34] M. Yoshida, T. Nakaura, T. Inoue et al., "Magnetic resonance cholangiopancreatography with GRASE sequence at 3.0 T: does it improve image quality and acquisition time as compared with 3D TSE?," *European Radiology*, vol. 28, pp. 2436–2443, 2018.

[35] T. M. Fiedler, M. E. Ladd, and A. K. Bitz, "SAR simulations & safety," *NeuroImage*, vol. 168, pp. 33–58, 2018.

[36] M. Okanovic, M. Völker, R. Trampel, F. Breuer, P. Jakob, and M. Blaimer, "Increasing robustness of radial GRASE acquisition for SAR-reduced brain imaging," *Zeitschrift für Medizinische Physik*, vol. 28, no. 3, pp. 236–246, 2018.

[37] M.-L. Chu, C.-P. Chien, W.-C. Wu, and H.-W. Chung, "Gradient-and spin-echo (GRASE) MR imaging: a long-existing technology that may find wide applications in modern era," *Quantitative Imaging in Medicine and Surgery*, vol. 9, no. 9, pp. 1477–1484, 2019.

[38] S. Dehghani, S. Shirani, and E. Jazayeri Gharehbagh, "Enhanced myocardial tissue visualization: a comparative cardiovascular magnetic resonance study of gradient-spin echo-STIR and conventional STIR imaging," *medRxiv*, 2023.